



Synergetic activation of H₂O₂ by photo-generated electrons and cathodic Fenton reaction for enhanced self-driven photoelectrocatalytic degradation of organic pollutants

Xia Li^{a,b}, Shanshan Liu^{a,b}, Di Cao^{a,b}, Ran Mao^{a,b}, Xu Zhao^{a,b,*}

^a Key Laboratory of Drinking Water Science and Technology, Research Center for Eco-Environmental Sciences, Chinese Academy of Sciences, Beijing, 100085, PR China

^b University of Chinese Academy of Sciences, Beijing, 100049, PR China



ARTICLE INFO

Keywords:
Photocatalytic fuel cell
Self-bias
H₂O₂ activation
Cathodic Fenton reaction
Recalcitrant organics

ABSTRACT

In this work, a self-driven photocatalytic fuel cell (PFC) system was constructed, which consisted of a noble metal-free Cu₂O/CuO photocathode and a semi-transparent BiVO₄ photoanode. The proposed PFC system was used for the degradation of phenol and the removal efficiency of phenol using BiVO₄-Cu₂O/CuO system was higher than the PFC using Pt cathode (BiVO₄-Pt, 67.3%) and bare Cu₂O cathode (BiVO₄-Cu₂O, 84.6%). The short circuit photocurrent of the BiVO₄- Cu₂O/CuO system was 0.30 mA cm⁻², which was higher than the sum of photocurrents generated by the other two photoelectrodes. This could be attributed to the self-driven bias induced by the good match of Fermi levels (E_F) between the BiVO₄ and the heterojunction Cu₂O/CuO electrode. The addition of 5 mM H₂O₂ to the PFC system greatly enhanced the degradation process, with the pseudo-first-order kinetic rate constant increased from 0.136 to 2.568 h⁻¹ after the addition of H₂O₂. Compared with traditional Fenton and Cu-based Fenton-like process, the PFC-H₂O₂ system has advantages of the broad working pH range (4–7), zero formation of ferric hydroxide sludge and less copper leaching. The X-ray photoelectron spectroscopy (XPS) analysis confirmed the cycle between Cu(I) and Cu(II) on the surface of Cu₂O/CuO photocathode, indicating that a Fenton-like reaction had occurred on Cu₂O/CuO photocathode. The H₂O₂ was activated by both the photo-generated electrons and the Cu₂O/CuO cathode, which further increased the degradation efficiency of phenol. Furthermore, a high stability was exhibited by the H₂O₂-PFC system.

1. Introduction

Photoelectrocatalytic (PEC) oxidation process has been intensively investigated, and has proved to be more efficient for the degradation of organic pollutants than individual photocatalysis and electrolysis processes [1–4]. In the PEC oxidation process, an external positive potential is employed on the semiconductor photoanode to drive the photo-generated electrons to migrate to the cathode, thus reducing the probability of electron/hole recombination [5]. However, the application of an external bias usually incurs use of additional energy, which increases the cost of the process [6]. Recently, photocatalytic fuel cell (PFC), which is a newly developed system for the simultaneous oxidation of organics and the generation of electricity from solar energy, has drawn significant research attentions [7–12]. In a PFC system, the photoelectrons are driven from anode to cathode due to the self-generated voltage rather than the applied external bias. Therefore, the need to apply additional external energy is avoided, which reduces the

overall energy consumption for the process.

Earlier PFC systems were used for the degradation of organic contaminants, and mainly consisted of TiO₂ photoanodes and Pt cathodes [13]. Gradually, the TiO₂ photoanodes were replaced with the visible light-responsive photoanodes [7,8,10,14,15]. More recently, the heterojunction photoanodes [16], such as BiVO₄/WO₃/W [11], TiO₂/g-C₃N₄ [17] and BiVO₄/TiO₂ [18] have been developed, and have exhibited higher catalytic activity in PFC systems. Besides the anodes, the cathodes used in PFCs have also undergone a rapid development. The Pt electrode used in traditional PFCs was expensive, and was not photo-responsive. Therefore, they have gradually been replaced with photocathodes in PFC systems. Recently, PFC systems with a dual photo-electrode were constructed and the mismatch of the Fermi levels between the photoanode and the photocathode was reported to be responsible for the generation of photovoltage in these PFC systems [15,18–20]. A visible light-driven PFC system is composed of a WO₃/W photoanode and a Cu₂O/Cu photocathode, and has been used for the

* Corresponding author at: Key Laboratory of Drinking Water Science and Technology, Research Center for Eco-Environmental Sciences, Chinese Academy of Sciences, Beijing, 100085, PR China.

E-mail address: zhaoxu@rcees.ac.cn (X. Zhao).

simultaneous degradation of organics and the electricity generation [19]. A PFC system with a TiO_2 photoanode and a $\text{C}/\text{Cu}_2\text{O}/\text{Cu}$ photocathode has been used to simultaneously treat wastewater and produce hydrogen [15]. Xia et al. reported a PFC system with a $\text{BiVO}_4/\text{WO}_3/\text{W}$ photoanode and a Pt modified commercial buried junction silicon (Pt/BJS) photocathode [11]. The Pt/BJS photocathode performed well in the PFC system. However, it is still desired to develop completely noble metal-free photoelectrodes.

Since the oxidation of organic pollutants in the PFC systems mainly occurred around the photoanode, an important factor that has limited their application in water treatment is their low efficiency and prolonged reaction time [8,19]. In PEC systems, the degradation efficiency of organics could be increased by strengthening the generation of radicals by adding either oxidizing agents or their precursors, such as H_2O_2 , persulfate and chloride ions [21–26]. In our previous work, persulfate was added in a UV- TiO_2 PEC system to enhance the PEC decomplexation of Cu-EDTA and Cu recovery [26]. A Fenton-PEC system was also reported, where feeding the Fe^{2+} cations strengthened the reaction of radicals and enhanced the degradation of organic pollutants [27]. Considering these works, it is highly possible that the performance of PFC systems for the degradation of organic pollutants could be enhanced by adding oxidizing substances.

In this study, a PFC system with dual photoelectrode was constructed using a noble metal-free photocathode and a nanostructured semi-transparent BiVO_4 photoanode. The $\text{BiVO}_4-\text{Cu}_2\text{O}/\text{CuO}$ PFC system was effective for the degradation of phenol under visible light. With the addition of 5 mM H_2O_2 , a 7-fold increase in the degradation efficiency of phenol was observed as compared with the individual PFC system. The added H_2O_2 was activated by the photo-generated electrons and the cathodic Fenton process, leading to the production of $\cdot\text{OH}$, which was responsible for the efficient degradation of phenol.

2. Experimental section

2.1. Materials

All the reagents with analytical grade were purchased from Sinopharm Chemical Reagent Co., Ltd and were used as received without further purification. The 5, 5-dimethyl-1-pyrrolidine-N-oxide (DMPO) and sulfamethoxazole were acquired from Aladdin, China. Fluorine-doped tin oxide (FTO) conductive film glasses with a size of $5 \times 2 \times 0.22$ cm were obtained from Shenzhen Jingweite Technology Co., Ltd. (Shenzhen, China). All aqueous solutions were prepared to a certain concentration with Milli-Q water ($18.2 \text{ M}\Omega \text{ cm}$).

2.2. Photoelectrode preparation and characterization

The BiVO_4 photoanode was prepared according to the previous report [28]. Briefly, a BiOI flake precursor was prepared on a FTO substrate by an electrodeposition method. Following, the prepared electrode was immersed into the DMSO solution of vanadium (IV) oxide bis (2, 4-pentanedionate) at 95°C . Finally, it was annealed in air at 450°C for 1 h.

The $\text{CuO}/\text{Cu}_2\text{O}$ cathode was prepared by electrodeposition followed by the annealing treatment in air [29,30]. Firstly, the electrodeposition of Cu_2O was performed potentiostatically with a potential of -0.3 V (vs. SCE) for 30 min at 60°C . The electrolyte was a mixture of 0.48 M copper sulfate and 3 M sodium lactate. The electrodeposition was conducted on a CHI660E electrochemical workstation (Chenhua Instrument Co. Ltd., Shanghai, China) using a three-electrode electrochemical cell, where FTO, Pt wire and Ag/AgCl electrode were used as working electrode, counter electrode and reference electrode, respectively. Then the prepared $\text{Cu}_2\text{O}/\text{FTO}$ was annealed at 400°C in air for 2 h and 4 h to obtain the $\text{CuO}/\text{Cu}_2\text{O}$ and CuO cathode.

The morphology of the photoelectrodes was characterized by field emission scanning electron microscopy (FE-SEM, Hitachi SU8020,

Tokyo, Japan). The crystalline structures of the samples were recorded on an X-ray diffractometer (XRD) (X'Pert Pro MPD) with a Cu K α radiation. UV-vis diffuse reflectance absorption spectra (UV-vis DRS) were recorded by Avalight DHS UV-vis absorbance measurements (Avantes, Netherlands). XPS spectra was measured using a PHI Quanta SXM instrument (ULVAC-PHI, Japan).

2.3. Photoelectrochemical experiments

The photoelectrochemical tests were carried out using a three-electrode cell with the prepared photoelectrodes, Pt wire and Ag/AgCl as working electrode, counter electrode and reference electrode, respectively. The working electrode parameters were controlled by a CHI660E potentiostat (CH Instruments, Inc.).

The PFC system was established using two-electrode configurations. The photoanode and photocathode were immersed in the solution in a quartz reactor and illuminated with one light source. Herein, a 300 W Xe lamp (PLS-SXE300; Perfect Light Co., Ltd, Beijing, China) with a 420 nm cutoff filter was used as light source (UVCUT420, $\lambda > 420$ nm). All the experiments were conducted in a quartz reactor (100 mL, $60 \times 30 \times 60$ mm.) with the same working area of the photoanode and photocathode of 4 cm^2 without applying the external potential. Degradation of the organic pollutants was carried out in a rectangular quartz reactor under a Xe lamp with a UV-cut filter ($\lambda > 420$ nm) irradiation. 0.1 M Na_2SO_4 was used as the electrolyte.

2.4. Analytical methods

The concentrations of phenol, bisphenol A and sulfamethoxazole were analyzed by a high performance liquid chromatography (HPLC, Shimadzu LC-20AT, Tokyo, Japan) equipped with a C18 column (GL Science Inc., Tokyo, Japan) and a UV detector. The mobile phase was a mixture of acetonitrile and water (V/V = 70/30) with a flow rate of 1 mL/min. The concentrations of Rhodamine B were analyzed by spectrophotometry method using UV-vis spectrometer (Hitachi U-3010). The TOC variation was measured by a multi N/C 3100 TOC/TNb analyzer (Analytikjena, Germany). Surface zeta potentials of BiVO_4 films were measured by Malvern Zetasizer Nano ZS90 at 30°C . For checking the involved active radicals, experiments were conducted on Bruker A300-10/12 (Germany) using DMPO as spin trapping agent. The measurements were carried out at the frequency of 9.85 GHz (X band), modulation of 100 kHz, and microwave power of 21 mW at room temperature. The generated $\cdot\text{OH}$ radicals were quantitatively analyzed using benzoic acid as probe molecule [31–33].

3. Results and discussion

3.1. Characterization of the photoelectrodes

Fig. 1a shows the XRD patterns and SEM image of the fabricated BiVO_4 photoanode. The BiVO_4 anode possessed a monoclinic scheelite crystal structure with the characteristic worm-like network morphology. Furthermore, the particles exhibited an average diameter of about 120 nm. The XRD patterns of the cathode are shown in **Fig. 1b**. The Cu_2O was electrodeposited onto the FTO substrate, whereas Cu_2O was partially oxidized to CuO after the annealing, indicating that the $\text{Cu}_2\text{O}/\text{CuO}/\text{FTO}$ electrode was formed. As can be seen from the SEM images in **Fig. 1c**, a compact layer of particles appeared on the Cu_2O electrode. The diameter of the particles was ~ 300 nm (**Fig. 1c**) and decreased to ~ 200 nm after annealing (**Fig. 1d**). The absorption edge of $\text{Cu}_2\text{O}/\text{FTO}$ and $\text{Cu}_2\text{O}/\text{CuO}/\text{FTO}$ estimated from UV-vis DRS is measured to be 600 nm and 900 nm (Fig. S1), respectively, indicating the enhanced absorption and utilization of light by the $\text{Cu}_2\text{O}/\text{CuO}/\text{FTO}$ electrode.

Fig. 2a shows the short circuit currents (J_{SC}) for the BiVO_4 -Pt and $\text{Pt-Cu}_2\text{O}/\text{CuO}$ systems under chopped light. The corresponding values are

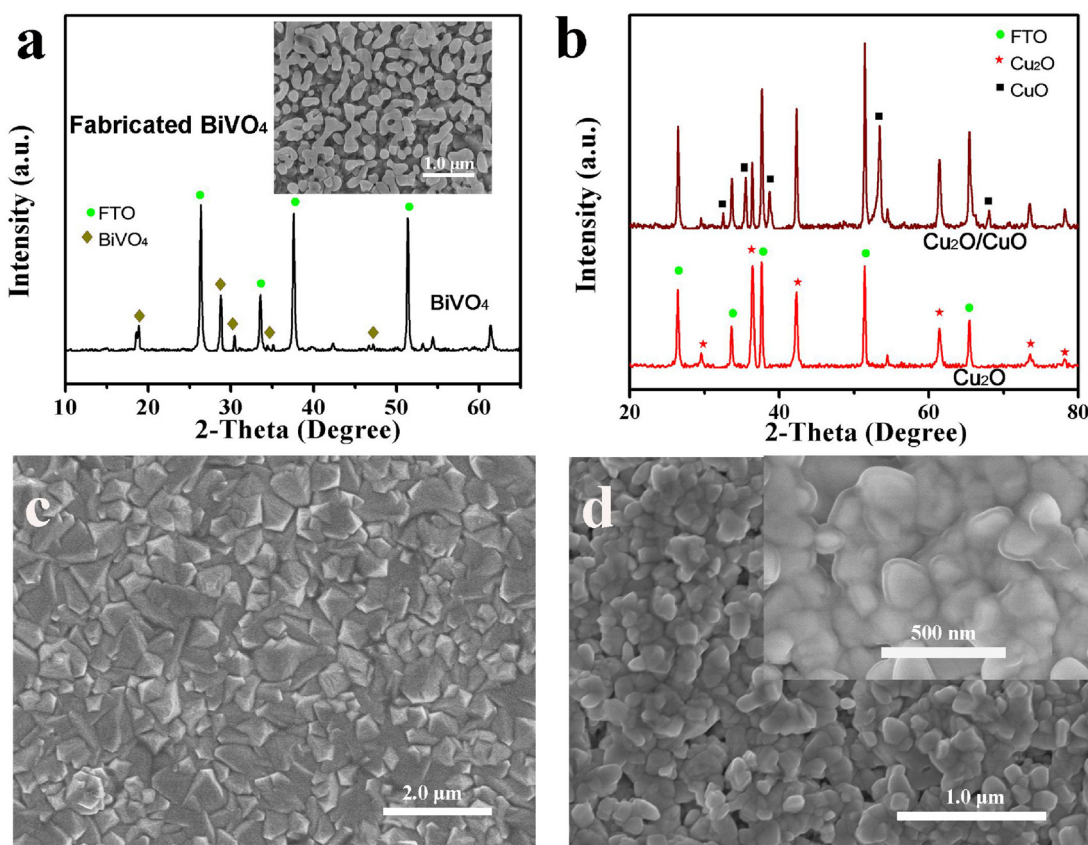


Fig. 1. (a) XRD pattern and SEM image (inset) of BiVO₄; (b) XRD patterns of Cu₂O and Cu₂O/CuO thin film electrodes; SEM images of Cu₂O (c), Cu₂O/CuO (d) [(c,d) top view].

0.10 and 0.15 mA cm⁻², respectively. By contrast, the J_{SC} of BiVO₄-Cu₂O/CuO system was measured to be 0.30 mA cm⁻², which was higher than the sum of photocurrents of the individual photoanode and photocathode, suggesting a synergistic effect between the photoanode and the photocathode. This effect may be caused by the mismatch of E_{PS} of the two electrodes [15]. Specifically, as shown in Fig. 2b, the photocurrent density of BiVO₄-Cu₂O/CuO PFC system was higher than that of the BiVO₄-Cu₂O PFC system (ca. 0.13 mA cm⁻²), indicating a higher photoelectrocatalytic activity of the CuO/Cu₂O electrode than that of the Cu₂O electrode. As shown in Fig. 2c, the charge transfer resistance (R_{ct}) values of the CuO/Cu₂O electrode were smaller than those of Cu₂O electrode (both in dark and illuminated conditions), suggesting that the CuO/Cu₂O heterojunction promotes the separation of photo-generated electrons and holes. To estimate the majority charge carrier density (N_A), the Mott-Schottky (M-S) plots of Cu₂O and Cu₂O/CuO electrodes were measured [34] (Fig. S2). The calculated N_A values of Cu₂O and Cu₂O/CuO were 6.46×10^{18} and 8.35×10^{19} cm⁻³, respectively. The higher majority charge carrier density of the CuO/Cu₂O indicated a higher rate of charge transfer and an enhanced photoelectrochemical performance. The details are presented in supporting information (SI) Text S1. In short, the increase of the photocurrent density indicated that the construction of heterojunction resulted in a faster charge transfer rate and a higher separation efficiency of the photo-generated electron-hole pairs.

3.2. Performance of PFC system for phenol degradation

Phenol was selected as a typical organic pollutant to evaluate the degradation performance of organics for the BiVO₄-Cu₂O/CuO PFC system. Fig. 3a shows the degradation efficiency of phenol in electrocatalysis (EC), photocatalysis (PC) and PFC systems, where EC refers to the wired configuration without light illumination, PC refers to the

wireless configuration with light illumination, and PFC presents the wired configuration with light illumination. Nearly no removal of phenol was observed for EC, whereas 33.2% of total phenol with an initial concentration of 5 mg/L was removed by the PC system. By contrast, for the PFC system, complete removal of phenol was achieved. These results demonstrated that the photocatalytic oxidation of organic contaminant can be greatly enhanced in the PFC system. The rate constant k for various systems was found in the following order: k_{PFC} (0.136 h⁻¹, $R^2 = 0.9542$) > k_{PC} (0.014 h⁻¹, $R^2 = 0.9920$) > k_{EC} (0.003 h⁻¹, $R^2 = 0.9896$). The rate constant of PFC system was almost 10-fold higher than that of the PC system, which may be attributed to the inhibition of the recombination of photo-generated electron-hole pairs due to the self-generated bias [11,35].

Among the PFC systems with three different cathodes, the degradation of phenol with CuO/Cu₂O cathode (BiVO₄-CuO/Cu₂O, 100%) was significantly higher than those with Pt cathode (BiVO₄-Pt, 67.3%) and single Cu₂O cathode (BiVO₄-Cu₂O, 84.6%) (Fig. 3b). The TOC removal also increased from 18.6% (BiVO₄-Pt) and 25.4% (BiVO₄-Cu₂O) to 40.3% (BiVO₄-CuO/Cu₂O) (Fig. 3b inset). These results indicate that the noble metal-free heterojunction photocathode is a promising option for organic pollutant degradation. Besides, as shown in Fig. 3c, the short-circuit current density curves of PFC systems remained nearly unchanged during the degradation process of phenol, indicating the high stability of the PFC system.

3.3. Enhanced phenol degradation in the presence of H₂O₂

As shown in Fig. 4a, with the addition of 5 mM H₂O₂, the removal efficiency of phenol increased from 15.2% to 100% within 2 h. The results showed that the degradation of phenol followed a pseudo-first-order kinetics. The variation of the rate constant with different H₂O₂ concentrations is shown in Fig. 4a inset. The reaction rate constant

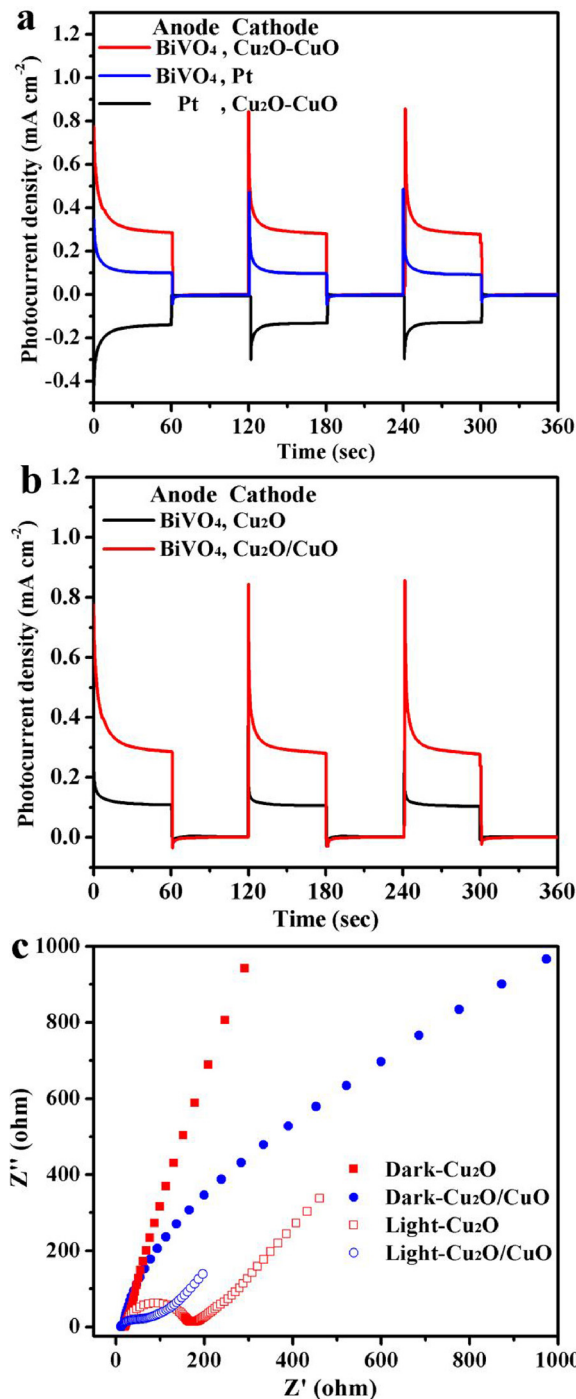


Fig. 2. (a) The photocurrent densities of various PFC systems and (b) the effect of CuO/Cu₂O heterojunction on the photocurrent densities of the PFC systems, where the substrate is 0.05 M phenol and support electrolyte is 0.1 M Na₂SO₄; (c) Nyquist plots of the Cu₂O and CuO/Cu₂O with and without visible light illumination, where the support electrolyte is 0.5 M Na₂SO₄.

increased from 0.136 h⁻¹ in the absence of H₂O₂ to 1.324 h⁻¹ (1 mM H₂O₂), 1.803 h⁻¹ (2 mM H₂O₂) and 2.568 h⁻¹ (5 mM H₂O₂), respectively. The TOC removal ratio also increased from 8.8% in the absence of H₂O₂ to 25.1% (1 mM H₂O₂), 34.9% (2 mM H₂O₂), and 44.6% (5 mM H₂O₂) (Fig. 4b). It can be seen from Fig. 4b inset that the J_{SC} of H₂O₂-PFC system increased with the increase in the concentration of H₂O₂. Besides, the removal ratio of single CuO/Cu₂O-H₂O₂ under visible light irradiation was only 8% (Fig. S3). All these results indicated that the introduction of H₂O₂ to PFC process increased the efficiency for phenol

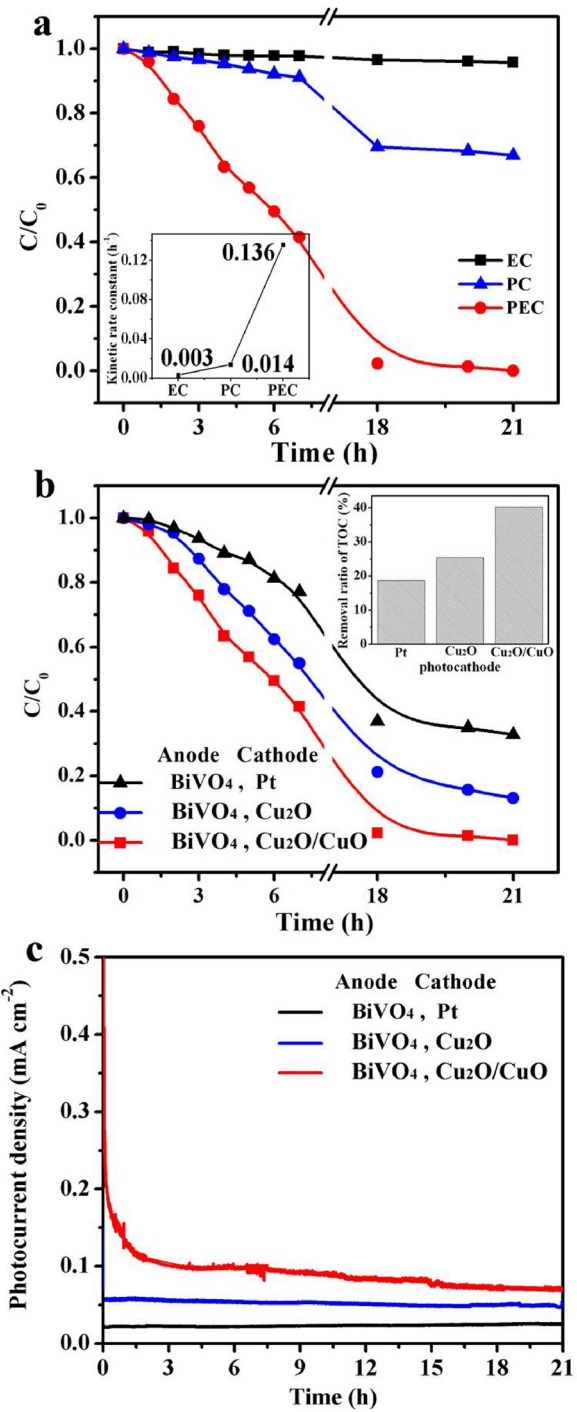


Fig. 3. (a) The removal of phenol and corresponding kinetic constants (inset) in different systems; (b) Phenol removal efficiency with various cathodes (inset Figure, TOC removal); (c) Variation of photocurrent densities in the phenol degradation process with three kinds of PFC systems using various photo-cathodes. Conditions: [phenol] = 5 mg/L; pH 6.0; $\lambda > 420$ nm.

degradation, and that phenol can be degraded more thoroughly in the currently proposed PFC process at higher H₂O₂ concentrations. Due to the difference between the Fermi levels of photoanode and photocathode [36–38], the photo-generated electrons on the BiVO₄ photoanode were driven to combine with the photo-generated holes on the CuO/Cu₂O photocathode. Therefore, the recombination of photo-generated electrons and holes on the photoanode and photocathode was effectively inhibited, which resulted in the enhancement of oxidation of organic contaminant on the BiVO₄ photoanode. When H₂O₂ was added

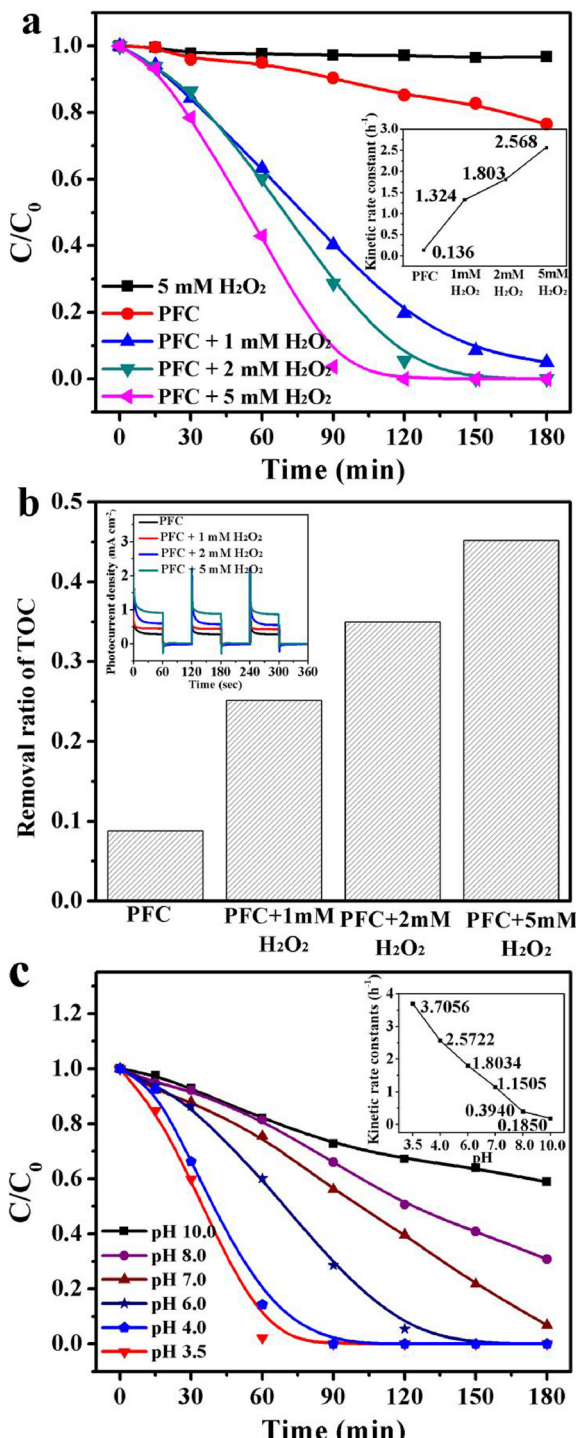
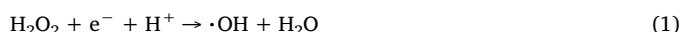


Fig. 4. (a) Effect of H_2O_2 concentration on phenol removal and corresponding kinetic constants (inset); (b) the removal ratio of TOC with $\text{pH} = 6.0$ and photocurrent densities (inset); (c) Effect of pH value on phenol removal and corresponding kinetic constants (inset) in the H_2O_2 -PFC system with 2 mM H_2O_2 addition. Conditions: [phenol] = 5 mg/L; $\lambda > 420 \text{ nm}$.

to the PFC system, the photo-generated electrons on the $\text{CuO}/\text{Cu}_2\text{O}$ photocathode activated H_2O_2 to generate $\cdot\text{OH}$ (Eq. (1)), which possesses strong oxidizing ability and efficiently degrades organic pollutants [39–42].



The effect of initial pH value on the degradation of phenol is

presented in Fig. 4c. The degradation efficiency of phenol was higher than 65% at 3 h for the pH values of less than 8.0. In contrast, only 38.5% of the total phenol was removed at pH 10.0. As can be seen from the inset of Fig. 4c, the degradation rate of phenol was in accordance with the pseudo-first-order reaction model, whereas the kinetic rate constants increased with the decrease in pH value. This can be explained by the difference of surface charge of BiVO_4 and the status of phenol at different pH values. The point of zero charge (pH_{pzc}) of BiVO_4 was measured to be 2.60 (Fig. S4). The pK_a of phenol is 9.95 [41]. At $\text{pH} > 9.95$, both the BiVO_4 and phenol were negatively charged, which made it difficult for phenol to be adsorbed on the surface of BiVO_4 due to the electrostatic repulsion. Therefore, low phenol degradation efficiency was observed at pH 10.0. When the pH lied in the range of 3.5–8.0, the BiVO_4 was negatively charged while phenol was mainly presented as neutral molecular specie. In consequence, the effect from the electrostatic repulsion can be precluded. There may be some other factors that played a dominant role in the degradation of phenol in the system. It was shown that phenol can be efficiently degraded even under acidic conditions. According to Eq. (1), at low pH, H^+ ions promoted the generation of $\cdot\text{OH}$, which was consistent with the results reported by Castillo et al [40].

The leaching of Cu with addition of 2 mM H_2O_2 was also measured for the pH_0 lying within the range of 3.5–10.0. The highest concentration of Cu was measured to be 0.65 mg/L at pH 3.5, which is much less than that of Cu-based H_2O_2 process (> 10 mg/L) [43–45]. The concentration of Cu decreased with the increase in pH_0 value. For pH values higher than 4.0, the concentration of Cu was less than 0.2 mg/L, and nearly no Cu was detected at pH values higher than 8.0 (Fig. S5). Given the removal efficiency of phenol and the leaching of Cu, the proper working pH range of PFC- H_2O_2 is 4–7. Previous researches have shown that Cu(I) and Cu(II) can act as catalysts for H_2O_2 activation in the degradation of various organic pollutants [42,46,47]. This Fenton-like reaction may also exist in the currently proposed H_2O_2 -PFC system, especially under acidic conditions.

3.4. Active species involved in the H_2O_2 -PFC system

As shown in Fig. 5a, for the currently proposed H_2O_2 -PFC system, phenol degradation was completely inhibited with the addition of *tert*-butyl alcohol (TBA), which is known as a scavenger of $\cdot\text{OH}$ radicals [48]. In the presence of ammonium oxalate (AO), a scavenger of photo-generated holes [49], the removal of phenol reduced from 100.0% to 49.1%. When the solution was purged with N_2 , which can be used as a scavenger for superoxide radical ($\cdot\text{O}_2^-$) [50], the degradation of phenol was decreased to 75.5%. These results indicate that $\cdot\text{OH}$, $\cdot\text{O}_2^-$ and photo-generated holes are all involved in the degradation of phenol, and $\cdot\text{OH}$ plays the major role. As can be seen from Fig. S6, the degradation of phenol in the PFC system without H_2O_2 decreased with the addition of TBA and AO and with the pumping of N_2 , although the drop in the degradation was relatively low. This result indicates that the PFC system may have the similar mechanism with the H_2O_2 -PFC system. As shown in Fig. 5b, the amount of $\cdot\text{OH}$ produced in the H_2O_2 -PFC system was 51.6 μM , which was about four times higher than that of the individual PFC system (without H_2O_2) (12.2 μM).

Furthermore, ESR spin-trapping technique that uses DMPO as the spin trapping agent was used to detect the generated active radicals. As shown in Fig. 5b inset, with the addition of H_2O_2 , the signal of DMPO- $\cdot\text{OH}$ adduct is enhanced significantly compared to the individual PFC system (without H_2O_2). As shown in Fig. 5c, $\cdot\text{OH}$ radicals were detected on both the $\text{Cu}_2\text{O}/\text{CuO}$ photocathode and the BiVO_4 photoanode in the proposed H_2O_2 -PFC system. In the PFC system, the electron-hole pairs were generated from the photoanode, while the holes moved to the surface of semiconductor to react with water to produce $\cdot\text{OH}$ [51]. The detected $\cdot\text{OH}$ radicals at the anode may have come from this process. The relative intensity of $\cdot\text{OH}$ radicals at the cathode was significantly higher than that at the anode and in the bulk solution, which suggested

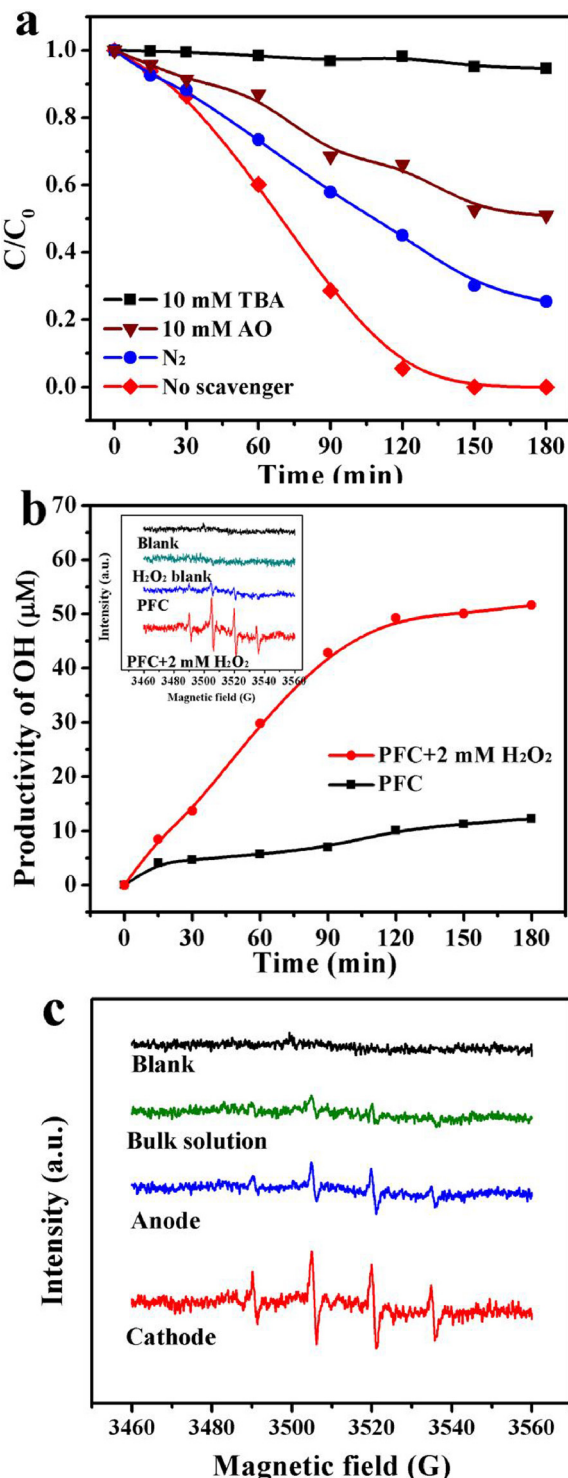


Fig. 5. (a) Effect of free radical inhibitors on the phenol removal efficiency in PFC- H_2O_2 system; (b) The productivity of ·OH in PFC and H_2O_2 -PFC systems and ESR spectra obtained in different system (inset); (c) Comparison of ESR spectrum in bulk solution, at the anode and at the cathode in H_2O_2 -PFC systems. Conditions: [phenol] = 5 mg/L; [H_2O_2] = 2 mM; pH 6.0; $\lambda > 420$ nm.

that most of the ·OH radicals were produced from the activation of H_2O_2 at the Cu_2O/CuO cathode.

3.5. Cathodic Fenton-like reaction for enhanced removal of phenol

To evaluate the role of cathode in the H_2O_2 -PFC system, the removal

of phenol with the addition of H_2O_2 to EC system was studied. The activation of H_2O_2 by photo-generated electrons was eliminated during the process. As shown in Fig. S7a, after the addition of H_2O_2 , the removal of phenol in the EC system increased from 0.05% to 4.2% within 3 h. It is worth noticing that the degradation of phenol in the EC system is enhanced significantly with the addition of H_2O_2 . As shown in the ESR spectrum (Fig. S7b), the signal of DMPO-·OH adduct enhanced significantly when H_2O_2 was added to the EC system. However, the current densities in the EC system remained nearly zero with the addition of 2 mM H_2O_2 (Fig. S7c), which indicated that the formation of ·OH from H_2O_2 in the EC system may have resulted from the 'Fenton-like' reaction between Cu(I) and H_2O_2 at the Cu_2O/CuO photocathode rather than by the electrochemically generated electrons [42,52,53].

To investigate the role of Cu_2O/CuO photocathode in the activation of H_2O_2 , the surface variation of the Cu_2O/CuO photocathode was studied using XRD, SEM and XPS analyses. The results showed that the surface of Cu_2O/CuO was uniform before the reaction (Fig. S8a inset). The particles on the surface of the cathode grew larger after the reaction. The XRD patterns of the cathode before and after the reaction are shown in Fig. S8a. The types of crystal structure of the cathode remained nearly unchanged after the reaction, whereas Cu_2O and CuO were still the main phases of the electrodes. The electrodes were further analyzed using the XPS technique. The major elements on the Cu_2O/CuO surface remained unchanged even after the reaction (Fig. S8b). Fig. 6 shows the XPS spectra of Cu 2p orbital for the Cu_2O/CuO photocathode at different reaction time. For Cu_2O/CuO during the reaction, the peaks were observed at 934.6 and 954.0 eV, respectively, and were assigned to Cu(II) of CuO [54]. Besides, the Cu species also existed in the state of Cu(I) (Cu_2O) as indicated by the two intense peaks observed at 932.7 and 952.5 eV [54–56]. These two peaks were assigned to Cu 2p3/2 and Cu 2p1/2 spin-orbital, respectively. It can be seen from Fig. 6 that the relative intensity of typical peaks for Cu(I) and Cu(II) vary with different reaction time. Cu(I) was oxidized to Cu(II) for the activation of H_2O_2 by Fenton-like reaction, which can be further reduced to Cu(I) by electrons on the cathode and continued to act as the catalyst. Thus the recycle of Cu(I) and Cu(II) can be realized on the Cu_2O/CuO photocathode surface during the reaction. Considering the important roles of Cu(I) in the H_2O_2 activation, it can be rationally inferred that Cu(I) and Cu(II) species on the photocathode surface acted as Fenton-like catalysts and contributed to the formation of ·OH following the reactions represented by Eqs. (2)–(5) [46].



3.6. Proposed mechanism

Based on above results, the mechanism of enhanced degradation of phenol with the addition of H_2O_2 has been proposed. Under the irradiation of visible light, the electron-hole pairs were generated on the $BiVO_4$ photoanode. The photo-generated h^+ oxidized water to generate ·OH through Eqs. (6) and (7). The photo-generated e^- were transferred to the photocathode through external circuit driven by the generated photovoltage. Meanwhile, the H^+ produced from the photo-oxidation of H_2O diffused towards the photocathode through the electrolyte solution. On the surface of photocathode, O_2 was reduced to H_2O through the arrival of electrons under conditions (Eq. (8)).



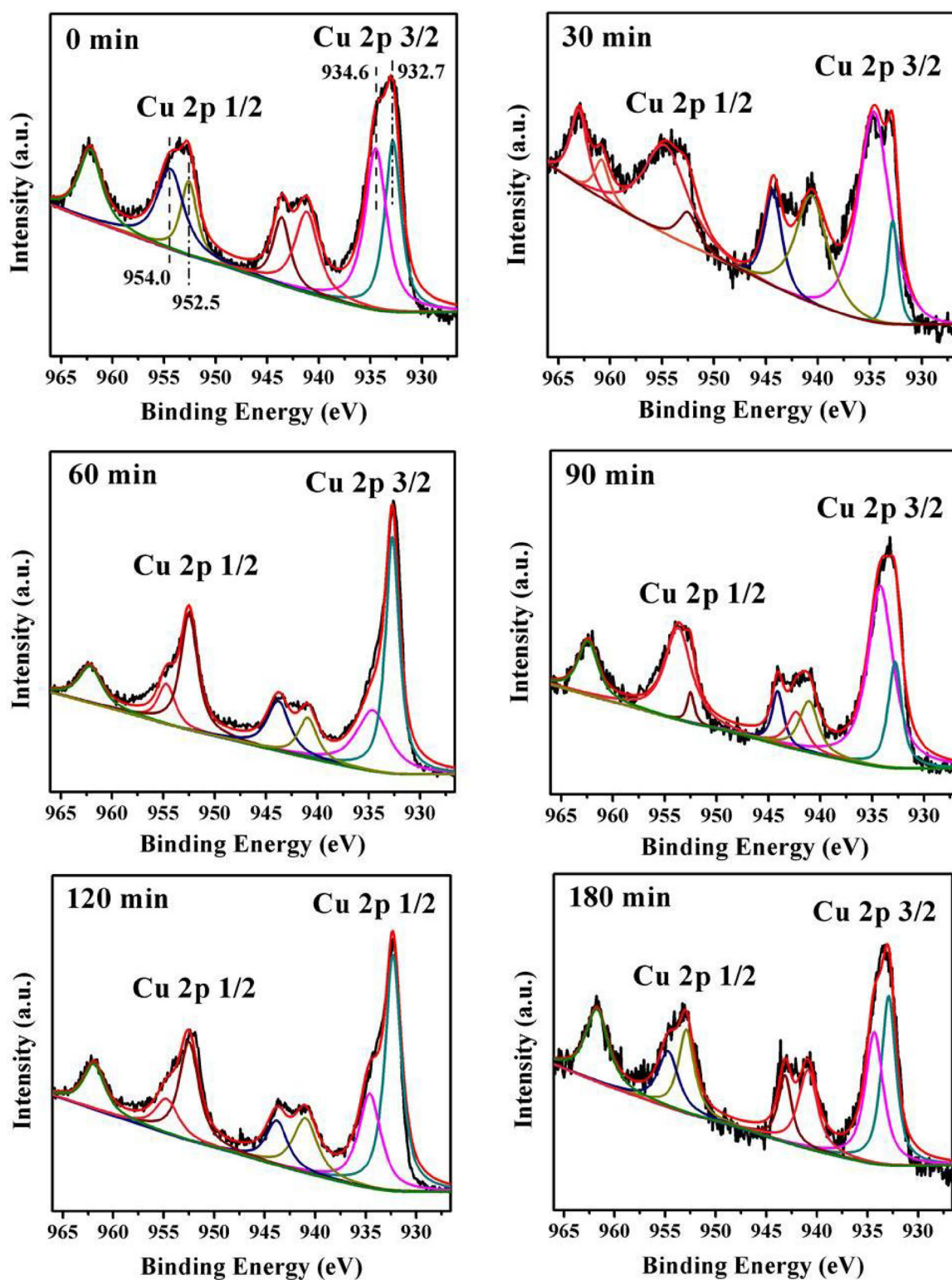
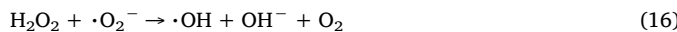


Fig. 6. XPS Cu 2p spectra of the photocathode at different reaction time. Conditions: [phenol] = 5 mg/L; [H₂O₂] = 2 mM; $\lambda > 420$ nm.

A current at the external circuit then generated due to the Fermi levels difference between the two photoelectrodes. At the cathode, radicals such as $\cdot\text{O}_2^-$, $\cdot\text{OH}$, and hydrogen superoxide radical ($\text{HO}_2\cdot$) were produced through the reduction of O_2 and H_2O_2 by e^- according to Eqs. (9)–(16) [40,41,57].





In the proposed H_2O_2 -PFC system, the added H_2O_2 strengthened the reactions of Eqs. (15) and (16), leading to a higher amount of $\cdot\text{OH}$ than that in the individual PFC system (without H_2O_2). Moreover, the “Fenton-like” reaction occurred at the $\text{Cu}_2\text{O}/\text{CuO}$ photocathode between Cu(I) and H_2O_2 (Eqs. (2)–(5)), leading to a more efficient formation of $\cdot\text{OH}$ radicals in the PFC system. As a result, the degradation of phenol was significantly increased.

The degradation of other recalcitrant organic pollutants including BPA, SMX and RhB were performed to further evaluate the performance of PFC systems. As shown in Fig. S9a, the values for the removal of PhOH, BPA, SMZ, and RhB in the individual PFC system (without H_2O_2) were measured to be 23.5%, 74.5%, 14.2%, and 62.3% within 3 h, respectively. After the addition of 2 mM H_2O_2 , the values for the removal of these contaminants increased to 100.0% (PhOH), 100.0% (BPA), 62.6% (SMZ), and 91.2% (RhB). These results confirmed the high efficiency of H_2O_2 -PFC system for the removal of recalcitrant organics removal. As shown in Fig. S9b, the removal efficiency of phenol remained nearly constant for three cycles in the proposed H_2O_2 -PFC system, indicating high stability and recyclability of the H_2O_2 -PFC system for the removal of organics.

4. Conclusion

In summary, a PFC system consisting of a noble metal-free $\text{Cu}_2\text{O}/\text{CuO}$ photocathode and a semi-transparent BiVO_4 photoanode was established, which exhibited activity towards phenol degradation under visible light irradiation with self-bias. Addition of H_2O_2 into the PFC system largely enhanced the degradation of organic contaminants, which was favored at low pH conditions. The active radicals of $\cdot\text{OH}$ was mainly responsible for organics degradation in the H_2O_2 -PFC system. H_2O_2 was jointly activated by the photogenerated electrons and the cathodic Fenton-like reaction at the $\text{Cu}_2\text{O}/\text{CuO}$ photocathode. Combined with the photoanodic oxidation, the targeted organics were efficiently oxidized.

Acknowledgements

This work was supported by National Natural Science Foundation of China (No. 21777176, 51578532).

Appendix A. Supplementary data

Supplementary material related to this article can be found, in the online version, at doi:<https://doi.org/10.1016/j.apcatb.2018.04.042>.

References

- [1] Z. Frontistis, V.M. Daskalaki, A. Katsaounis, I. Poulios, D. Mantzavinos, Water Res. 45 (2011) 2996–3004.
- [2] K. Li, Y. He, Y. Xu, Y. Wang, J. Jia, Environ. Sci. Technol. 45 (2011) 7401–7407.
- [3] T. An, H. Sun, G. Li, H. Zhao, P.K. Wong, Appl. Catal. B-Environ. 188 (2016) 360–366.
- [4] Y.-P. Peng, H. Chen, C.P. Huang, Appl. Catal. B-Environ. 209 (2017) 437–446.
- [5] X. Meng, Z. Zhang, X. Li, J. Photochem. Photobiol. C Photochem. Rev. 24 (2015) 83–101.
- [6] N. Andrews, J. Willis, C. Muller, Assess. Technol. Adv. Future Energy Reduct. (2016).
- [7] M. Antoniadou, P. Lianos, Photochem. Photobiol. Sci. 10 (2011) 431.
- [8] J. Li, J. Li, Q. Chen, J. Bai, B. Zhou, J. Hazard. Mater. 262 (2013) 304–310.
- [9] Y. Liu, J. Li, B. Zhou, X. Li, H. Chen, Q. Chen, Z. Wang, L. Li, J. Wang, W. Cai, Water Res. 45 (2011) 3991–3998.
- [10] Y. Liu, J. Li, B. Zhou, S. Lv, X. Li, H. Chen, Q. Chen, W. Cai, Appl. Catal. B-Environ. 111 (2012) 485–491.
- [11] L. Xia, J. Bai, J. Li, Q. Zeng, X. Li, B. Zhou, Appl. Catal. B-Environ. 183 (2016) 224–230.
- [12] K. Zhao, J. Bai, Q. Zeng, Y. Zhang, J. Li, L. Li, L. Xia, B. Zhou, J. Hazard. Mater. 337 (2017) 47–54.
- [13] M. Kaneko, J. Nemoto, H. Ueno, N. Gokan, K. Ohnuki, M. Horikawa, R. Saito, T. Shibata, Electrochim. Commun. 8 (2006) 336–340.
- [14] Y. Liu, J. Li, B. Zhou, H. Chen, Z. Wang, W. Cai, Chem. Commun. 47 (2011) 10314–10316.
- [15] Z. Wu, G. Zhao, Y. Zhang, J. Liu, Y.-n. Zhang, H. Shi, J. Mater. Chem. A. 3 (2015) 3416–3424.
- [16] Z. Bian, F. Cao, J. Zhu, H. Li, Environ. Sci. Technol. 49 (2015) 2418–2424.
- [17] T. Yu, L. Liu, F. Yang, Chin. J. Catal. (2017) 270–277.
- [18] J. Bai, R. Wang, Y. Li, Y. Tang, Q. Zeng, L. Xia, X. Li, J. Li, C. Li, B. Zhou, J. Hazard. Mater. 311 (2016) 51–62.
- [19] Q. Chen, J. Li, X. Li, K. Huang, B. Zhou, W. Cai, W. Shangguan, Environ. Sci. Technol. 46 (2012) 11451–11458.
- [20] M.G. Walter, E.L. Warren, J.R. McKone, S.W. Boettcher, Q.X. Mi, E.A. Santori, N.S. Lewis, Chem. Rev. 110 (2010) 6446–6473.
- [21] B.J. Hernlem, Water Res. 39 (2005) 2245–2252.
- [22] M. Panizza, G. Cerisola, Electrochim. Acta. 48 (2003) 1515–1519.
- [23] H.X. Shi, J.H. Qu, A.M. Wang, J.T. Ge, Chemosphere 60 (2005) 326–333.
- [24] H.B. Zeng, S.C. Tian, H.F. Liu, B.Y. Chai, X. Zhao, Chem. Eng. J. 301 (2016) 371–379.
- [25] S.S. Liu, X. Zhao, H.B. Zeng, Y.B. Wang, M. Qiao, W. Guan, Chem. Eng. J. 320 (2017) 168–177.
- [26] H.B. Zeng, S.S. Liu, B.Y. Chai, D. Cao, Y. Wang, X. Zhao, Environ. Sci. Technol. 50 (2016) 6459–6466.
- [27] K. Zhao, Q. Zeng, J. Bai, J. Li, L. Xia, S. Chen, B. Zhou, Water Res. 108 (2017) 293–300.
- [28] Y.B. Kuang, Q.X. Jia, H. Nishiyama, T. Yamada, A. Kudo, K. Domen, Adv. Energy Mater. 6 (2016) 1–7.
- [29] K.H. Han, M. Tao, Sol. Energy Mater. Sol. Cells. 93 (2009) 153–157.
- [30] P. Wang, H. Wu, Y.M. Tang, R. Amal, Y.H. Ng, J. Phys. Chem. C 119 (2015) 26275–26282.
- [31] X. Zhou, K. Mopper, Mar. Chem. 30 (1990) 71–88.
- [32] M.E. Lindsey, M.A. Tarr, Chemosphere 41 (2000) 409–417.
- [33] S.H. Joo, A.J. Feitz, D.L. Sedlak, T.D. Waite, Environ. Sci. Technol. 39 (2005) 1263–1268.
- [34] Y. Yang, D. Xu, Q.Y. Wu, P. Diao, Sci. Rep. 6 (2016) 1–13.
- [35] P. Lianos, Appl. Catal. B-Environ. 210 (2017) 235–254.
- [36] G. Li, Y. Bai, W.F. Zhang, Mater. Chem. Phys. 136 (2012) 930–934.
- [37] R.P. Wijesundera, M. Hidaka, K. Koga, J.Y. Choi, N.E. Sung, Ceram. Silikaty. 54 (2010) 19–25.
- [38] W.J. Yin, S.H. Wei, M.M. Aljassim, J. Turner, Y. Yan, Phys. Rev. B. 83 (2011) 970–978.
- [39] M. Saquib, M.A. Tariq, M.M. Haque, M. Muneer, J. Environ. Manag. 88 (2008) 300–306.
- [40] N.C. Castillo, L. Ding, A. Heel, T. Graule, C. Pulgarin, J. Photochem. Photobiol. A Chem. 216 (2010) 221–227.
- [41] C.-H. Chiou, C.-Y. Wu, R.-S. Juang, Sep. Purif. Technol. 62 (2008) 559–564.
- [42] H. Lee, H.J. Lee, D.L. Sedlak, C. Lee, Chemosphere 92 (2013) 652–658.
- [43] J.K. Kim, F. Martinez, I.S. Metcalfe, Catal. Today 124 (2007) 224–231.
- [44] Y. Zhan, X. Zhou, B. Fu, Y. Chen, J. Hazard. Mater. 187 (2011) 348–354.
- [45] S.B. Hammouda, F. Zhao, Z. Safaei, I. Babu, D.L. Ramasamy, M. Sillanpää, Appl. Catal. B-Environ. 218 (2017) 119–136.
- [46] A.N. Pham, G. Xing, C.J. Miller, T.D. Waite, J. Catal. 301 (2013) 54–64.
- [47] M.U. Prathap, B. Kaur, R. Srivastava, J. Colloid Interface Sci. 370 (2012) 144–154.
- [48] A.A. Burbano, D.D. Dionysiou, M.T. Suidan, T.L. Richardson, Water Res. 39 (2005) 107–118.
- [49] S. Li, D. Meng, L. Hou, D. Wang, T. Xie, Appl. Surf. Sci. 371 (2016) 164–171.
- [50] X.U. Shoubin, L. Jiang, H. Yang, Y. Song, D. Yi, Chin. J. Catal. 32 (2011) 536–545.
- [51] R. Daghrir, P. Drogui, D. Robert, J. Photochem. Photobiol. A Chem. 238 (2012) 41–52.
- [52] Y. Feng, P.H. Lee, D. Wu, Z. Zhou, H. Li, K. Shih, J. Hazard. Mater. 331 (2017) 81–87.
- [53] C. Toparli, A. Sarfraz, A.D. Wieck, M. Rohwerder, A. Erbe, Electrochim. Acta. 236 (2017) 104–115.
- [54] M.Q. Cai, Y.Z. Zhu, Z.S. Wei, J.Q. Hu, S.D. Pan, R.Y. Xiao, C.Y. Dong, M.C. Jin, Sci. Total Environ. 580 (2017) 966–973.
- [55] G. Nie, Z. Li, X. Lu, J. Lei, C. Zhang, C. Wang, Appl. Surf. Sci. 284 (2013) 595–600.
- [56] Y. Wang, H. Zhao, M. Li, J. Fan, G. Zhao, Appl. Catal. B-Environ. 147 (2014) 534–545.
- [57] W. Cui, J. Li, F. Dong, Y. Sun, G. Jiang, W. Cen, S.C. Lee, Z. Wu, Environ. Sci. Technol. 38 (2017) 10746–10753.